

Novel Design of Intersample Predictor Based on Multirate GPC for High-Speed Visual Servoing

Jiun-De Wu* Student Member
Yoichi Hori** Member

Visual servo system is a rapidly maturing approach to the control of robot manipulators that is based on visual recognition of robot and workpiece location. The role of computer vision as the feedback transducer strongly affects the closed-loop dynamics of the overall system. However, researches on visual servo system have up to date focused mainly on preview control (known trajectory), only a few papers have focused on prediction control (unknown trajectory). All of them have not considered coordinate transformation problem caused from the multirate characteristics of visual servo system while performing a high speed tracking.

In this paper, a novel visual servo prediction control scheme is proposed for achieving high speed tracking and high control accuracy. In view of the long time-delay and coordinate transformation problem caused by high speed motion, the use of an intersample predictor based on Multirate Generalized Predictive Control (GPC) is proposed to take care of external uncertainties and compute the optimal intersample control inputs of the robotic system. Finally, simulation and experimental results are given to show the drastic effectiveness of proposed approach.

Keywords: Visual Servoing, Generalized Predictive Control, Prediction Control, Multirate Control

1. Introduction

Traditional robot control is only based on the information from internal sensor, i.e. the angle encoder. Autonomous work operation in uncertain environment is impossible. Computer vision gives robots the ability to manipulate parts with uncertain characteristics and locations. One of the most important applications is vision-based material handling. Besides, In ITS(Intelligent Transportation System), a monitoring system which can track a specific object from vision is necessary. As a consequence, no matter what form the target motion takes on, linear, circular or sinusoidal trajectory, it must be able to be estimated and predicted with sufficient accuracy. Thus we are confronted with a control problem of tracking a mobile target with the help of dynamic visual feedback.

A conventional visual servo control diagram is shown in Fig.1. Two feedback loops are in this system. One is vision loop and another one is joint servo loop. However, the sampling period, T_f of vision sensor such as a CCD camera is comparatively slow(over 33ms), the control period, T_j of joint servo is fast(less than 1ms).

Computer vision has a number of significant disadvantages when used as a feedback sensor: a relatively low sampling rate, sensitive to variations of the environment illumination and coarse quantization. As a result, direct use of the visual data for robot control will lead to poor control accuracy.

Corke⁽¹⁾ et al. were the first that studied the effect of the manipulator's dynamics in the visual loop. Hashimoto^{(2) (3)} et al. proposed observer-based con-

troller to overcome delay and nonlinear dynamics. Gangloff^{(4) (5)} et al. were the first that implemented GPC on line to take into account the dynamics of the manipulator. Some multirate visual servoing approaches^{(6) (7)} based on preview control were also proposed. However, no author focused on the coordinate transformation problem caused by high speed tracking in visual servo prediction control. Our proposal is to overcome this problem using an intersample predictor based on multirate GPC⁽⁹⁾.

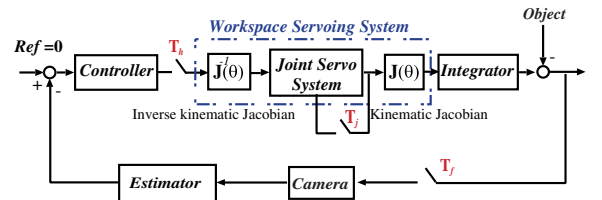


Fig. 1. Visual servo control system

2. Coordinate transformation problem in modeling the visual servo loop

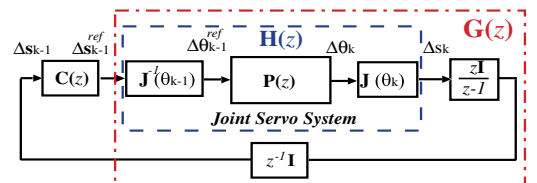


Fig. 2. Linearized dynamical model of the visual servo system

2.1 Analysis of Position-Based Visual Servo Control Before designing a controller, we have to derive a transfer function from the visual servo system shown in Fig.2.

In modeling the robot dynamics, we linearize this model by considering that the nonlinear effects act like

* Department of Electrical Engineering, Graduate School of Engineering, The University of Tokyo

** Information and System Division, Electrical Control System Engineering, Institute of Industrial Science, The University of Tokyo

slow load disturbances on the joint loop. The assumption is validated through the linear identification of an industrial manipulator.

The transfer functions between $\dot{\theta}^{ref}$ and $\dot{\theta}$ can be identified using classical identification techniques. Let $P_l(z)$ be the discrete time transfer function.

$$P_l(z) = \dot{\theta}_l / \dot{\theta}_l^{ref} \quad l = 1, \dots, n \quad (1)$$

where P_l are normalized by assuming that $\lim_{z \rightarrow 1} P_l(z) = 1$. Now suppose that kinematic Jacobian, \mathbf{J} and inverse kinematic Jacobian, \mathbf{J}^{-1} are given by

$$\mathbf{J}(\theta_k) = \begin{bmatrix} \mathbf{J}_{11} & \dots & \mathbf{J}_{1n} \\ \vdots & \ddots & \vdots \\ \mathbf{J}_{n1} & \dots & \mathbf{J}_{nn} \end{bmatrix}, \quad \mathbf{J}^{-1}(\theta_{k-1}) = \begin{bmatrix} \mathbf{J}_{11}^{-1} & \dots & \mathbf{J}_{1n}^{-1} \\ \vdots & \ddots & \vdots \\ \mathbf{J}_{n1}^{-1} & \dots & \mathbf{J}_{nn}^{-1} \end{bmatrix} \quad (2)$$

Moreover, the discrete open loop transfer function $\mathbf{G}(z)$ can be written as

$$\mathbf{G}(z) = \frac{\mathbf{I} - z\mathbf{I}}{z - \mathbf{I}} \mathbf{H}(z), \quad \mathbf{H}(z) = \mathbf{J}(\theta_k) \mathbf{P}(z) \mathbf{J}^{-1}(\theta_{k-1}) \quad (3)$$

Using $\mathbf{G}(z)$, we can design a controller for the visual servo system.

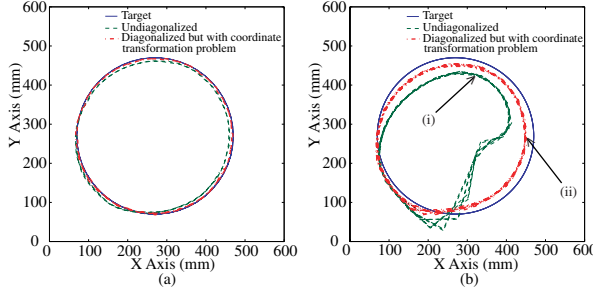


Fig. 3. (a) Low speed tracking $1\pi[\text{rad/s}]$ (b) High speed tracking $3\pi[\text{rad/s}]$

2.2 Coordinate transformation problem

In former subsection, we know if \mathbf{H} can be diagonalized by

$$\lim_{z \rightarrow 1} \mathbf{H}(z) = \mathbf{I} \quad (4)$$

we can design controller for each joint individually. But, if it is not, the controller design problem will become sophisticated and the calculation load will become drastically because of its updating every sampling period^{(4) (5)}. In past, in order to avoid this problem, to consider the sampling interval is short enough so that the target and the robot moves only a little during this interval and assume that \mathbf{J} is constant between two sampling instants is a well-known method. That is to say, if $\|\theta_k - \theta_{k-1}\| \approx 0$, then $\mathbf{H}(z)$ can be diagonalized appropriately (see Fig.3(a)). Actually, in industrial applications, i.e. a material handling robot workstation, wide-area operation and high speed moving are always the case, therefore, $\|\theta_k - \theta_{k-1}\| \neq 0$, $\mathbf{H}(z)$ cannot be diagonalized to \mathbf{I} .

To update the J^{-1} and J in servo loop sampling rate (see Fig.4(a)) is another approach. Although when equation(4) is satisfied in order to solve the serious diagonalized problem (see (i) in Fig.3(b)) but oppositely wrong coordinate transformation $\mathbf{J}^{-1}(\theta_{k-1+\nu_i}) \Delta \mathbf{s}_{k-1}^{ref} \neq \mathbf{J}^{-1}(\theta_{k-1}) \Delta \mathbf{s}_{k-1}^{ref}$ will occur during T_f (see (ii) in

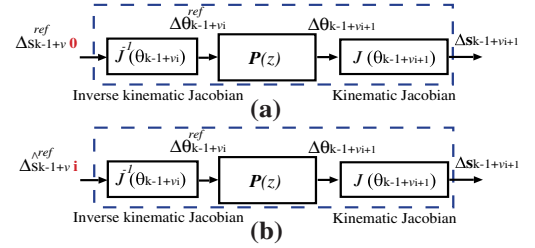


Fig. 4. (a) Inaccurate (b) Accurate workspace servo system

Fig.3(b)). Therefore, the positioning error will accumulate and finally result in poor control accuracy. Here, ν_i means $i \times \nu T_f$ where νT_f is the control period of joint loop.

3. Proposed Visual Servo Control Scheme

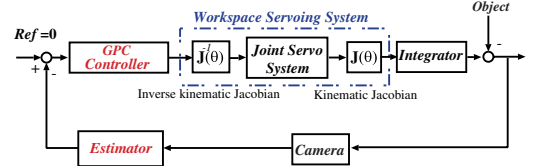


Fig. 5. Conventional visual servo control scheme

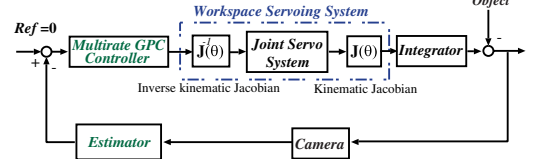


Fig. 6. Proposed visual servo control scheme

In former section, we have mentioned about some problems that will occur while performing a high speed visual servo control. In this section we will explain the proposed visual servo control scheme.

If we can design a control scheme as Fig.4(b). The following two relational expressions will be satisfied. Thus we can solve both the diagonalized problem and coordinate transformation problem appropriately at the same time. It also means we need an intersample predictor to implement this idea.

Diagonalizing :

$$\lim_{z \rightarrow 1} \mathbf{J}(\theta_{k-1+\nu_i+1}) \mathbf{P}(z) \mathbf{J}^{-1}(\theta_{k-1+\nu_i}) \approx \mathbf{I} \quad (5)$$

Accuracy coordinate transformation :

$$\theta_{k-1+\nu_i}^{ref} = \mathbf{J}^{-1}(\theta_{k-1+\nu_i}) \Delta \hat{\mathbf{s}}_{k-1+\nu_i}^{ref} \quad (6)$$

In conventional visual servo control^{(4) (5)} (see Fig.5), it needs to update controller every sampling period. In this paper, we design an intersample predictor based on multirate GPC using discrete-time lifting to let the control period of vision loop equal to intersample prediction period. Consequently, our proposed control system (see Fig.6) can satisfy both equation(5) and equation(6) and then solve the mentioned problems while performing a high-speed visual servo control. Moreover, the calculation load will be reduced drastically because we only have to calculate it once off-line.

3.1 Target state estimation

Studies on target

state estimates based on Luenberger observer, $\alpha - \beta - \gamma$ filter, Kalman filter, AR model were carried out by many authors⁽¹⁾. In this paper, we used a 3-order model based on Taylor series incorporated into Kalman filter to estimate target state.

In discrete-time state-space form the target dynamics are

$$\mathbf{x}_{k+1} = \mathbf{F}\mathbf{x}_k + \omega_k \dots \dots \dots (7)$$

$$y_k = \mathbf{H}\mathbf{x}_k + \nu_k \dots \dots \dots (8)$$

The vectors ω_k and ν_k are the process noise sequence with covariance \mathbf{Q} and the measurement noise sequence with covariance \mathbf{R} respectively.

The state-transition matrix \mathbf{F} and the observation matrix \mathbf{H} are

$$\mathbf{F} = \begin{bmatrix} 1 & T_f & \frac{T_f^2}{2!} \\ 0 & 1 & T_f \\ 0 & 0 & 1 \end{bmatrix}, \mathbf{H} = [1 \ 0 \ 0] \dots \dots \dots (9)$$

where T_f is the sampling period of vision sensor, the frame period.

For each Cartesian coordinate, the Kalman filter is given by

$$\hat{\mathbf{x}}_{k/k} = \hat{\mathbf{x}}_{k/k-1} + \mathbf{K}_k[y_k - \mathbf{H}\hat{\mathbf{x}}_{k/k-1}] \dots \dots \dots (10)$$

$$\mathbf{P}_{k/k} = \mathbf{P}_{k/k-1} - \mathbf{K}_k\mathbf{H}\mathbf{P}_{k/k-1} \dots \dots \dots (11)$$

$$\mathbf{K}_k = \mathbf{P}_{k/k-1}\mathbf{H}^T[\mathbf{H}\mathbf{P}_{k/k-1}\mathbf{H}^T + \mathbf{R}]^{-1} \dots \dots \dots (12)$$

$$\hat{\mathbf{x}}_{k+1/k} = \mathbf{F}\hat{\mathbf{x}}_{k/k} \dots \dots \dots (13)$$

$$\mathbf{P}_{k+1/k} = \mathbf{F}\mathbf{P}_{k/k}\mathbf{F}^T + \mathbf{Q} \dots \dots \dots (14)$$

where $\hat{\mathbf{x}}_{k/k}$ is the optimal target state estimation at time k .

3.2 Intersample Predictor Based on Multirate GPC

Traditionally, GPC has been derived using a transfer function model through Diophantine equations^{(4) (5)}. Here, we consider a state space formulation, which has the advantage that taking discrete-time lifting⁽⁸⁾ to be a multirate form is straightforward.

GPC is a control strategy that uses knowledge of the future behavior of the output for calculating the feedback signal. That is to say, it generates a sequence of future control signals within each sampling interval to optimize the control effort of the controlled system. We utilize this particular characteristic to design an intersample predictor. Let's lift variables, then lifted GPC can generate a sequence of future intersample control signals within each sampling interval.

Consider a controllable and observable LTI system represented in discrete time by

$$\begin{aligned} \mathbf{x}_{k+\nu_j+1} &= \mathbf{A}\mathbf{x}_{k+\nu_j} + \mathbf{B}\Delta\mathbf{u}_{k+\nu_j} + \mathbf{E}\mathbf{d}_{k+\nu_j} \\ \mathbf{y}_{k+\nu_j} &= \mathbf{C}\mathbf{x}_{k+\nu_j} \dots \dots \dots (15) \end{aligned}$$

where $\mathbf{A}, \mathbf{B}, \mathbf{C}$ are derived from $\mathbf{G}(z)$ in equation(3) using sampling time νT_f , $\nu = T_f/N$, $\nu_i = \frac{T_f}{N} \times i$, N is the intersample prediction input times during T_f . Here we consider the target motion act as the disturbance, $\mathbf{d}_{k+\nu_j}$, included in system.

Let's solve recursively, the following j -step future output prediction can be derived. Since the spectral properties of disturbances are unknown(arbitrary target motion), we remove them and then the minimum variance

estimator of $\mathbf{y}_{k+\nu_j}$ is given by

$$\hat{\mathbf{y}}_{k+\nu_j} = \mathbf{C}\mathbf{A}^j\mathbf{x}_k + \sum_{i=0}^{j-1} \mathbf{C}\mathbf{A}^{j-i-1}\mathbf{B}\Delta\mathbf{u}_{k+\nu_i} \dots \dots (16)$$

The objective of the GPC is to synthesize a set of optimal control input increments $\Delta\mathbf{u}_{k+\nu_{i-1}}$, $i = 1, \dots, N_u$. Using equation(16), we can obtain the following cost function.

$$\begin{aligned} J &= \sum_{j=N_1}^{N_2} \mathbf{e}_{k+\nu_j}^T \mathbf{e}_{k+\nu_j} + \lambda \sum_{i=1}^{N_u} \Delta\mathbf{u}_{k+\nu_{i-1}}^T \Delta\mathbf{u}_{k+\nu_{i-1}} \\ &= (\hat{\mathbf{Y}}_k - \mathbf{Y}_k^*)^T (\hat{\mathbf{Y}}_k - \mathbf{Y}_k^*) + \lambda \Delta\mathbf{U}_k^T \Delta\mathbf{U}_k \dots (17) \end{aligned}$$

where $\mathbf{e}_{k+\nu_j}$ is the future j -step predicted tracking error $\mathbf{e}_{k+\nu_j} = \hat{\mathbf{y}}_{k+\nu_j} - \mathbf{y}_{k+\nu_j}^*$, N_1, N_2 and N_u are the minimum, maximum and control costing horizons respectively, λ is the constant control input costing factor, $\mathbf{y}_{k+\nu_j}^*$ is the future reference.

Finally, by minimizing cost function, we can obtain the following optimal control increments:

$$\Delta\mathbf{U}_k = (\mathbf{G}^T\mathbf{G} + \lambda\mathbf{I})^{-1}\mathbf{G}^T(\mathbf{Y}_k^* - \Phi\mathbf{x}_k) \dots \dots \dots (18)$$

where

$$\hat{\mathbf{Y}}_k = [\hat{\mathbf{y}}_{k+\nu_{N_1}}, \dots, \hat{\mathbf{y}}_{k+\nu_{N_2}}]^T \dots \dots \dots (19)$$

$$\Delta\mathbf{U}_k = [\Delta u_k, \dots, \Delta u_{k+\nu_{N_u-1}}]^T \dots \dots \dots (20)$$

$$\mathbf{Y}_k^* = [\mathbf{y}_{k+\nu_{N_1}}^*, \dots, \mathbf{y}_{k+\nu_{N_2}}^*]^T \dots \dots \dots (21)$$

In our case, the camera configuration is end-effector mounted. So the reference should always be 0 for target tracking, $\mathbf{Y}_k^* = \mathbf{0}$.

Then the intersample optimal control inputs can be obtained by the following equations.

$$\Delta u_k = [1, 0, \dots, 0] \Delta\mathbf{U}_k \dots \dots \dots (22)$$

$$\Delta u_{k+\nu_1} = [0, 1, \dots, 0] \Delta\mathbf{U}_k \dots \dots \dots (23)$$

\vdots

$$\Delta u_{k+\nu_{N-1}} = [0, 0, \dots, 1] \Delta\mathbf{U}_k \dots \dots \dots (24)$$

4. Simulations and experiments

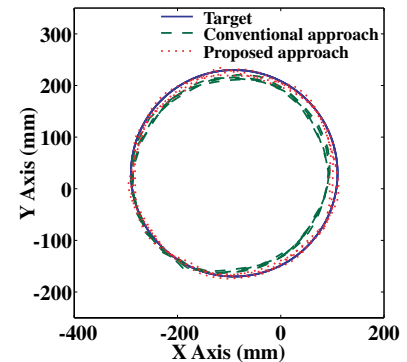


Fig. 7. Tracking trajectory(simulation)

4.1 Simulation results In this simulation, the initial position of the target is $(-90, 30)$, target will start a circular movement with radius $200[mm]$, $\omega = 2\pi[rad/s]$ at $t = 2.0$. The sampling period of vision

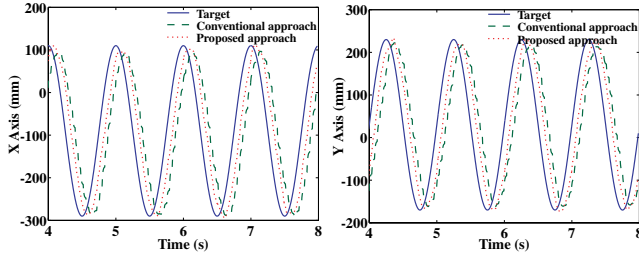


Fig. 8. Tracking response(simulation)

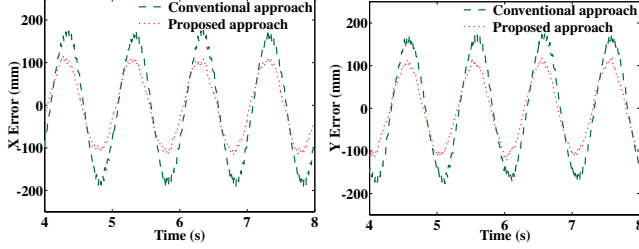


Fig. 9. Tracking error(simulation)

sensor is $40[ms]$. The comparison approach is the visual control scheme proposed in ⁽⁴⁾ ⁽⁵⁾, incorporated a Kalman filter. Fig.7, Fig.8 and Fig.9 show that the proposed approach has higher control accuracy and higher prediction performance than conventional approach.

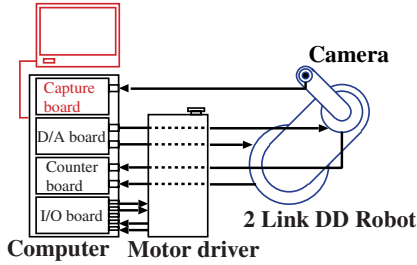


Fig. 10. Experimental setup

4.2 Experimental results In the experiments, a two-link direct drive robot is utilized(see Fig.10), and a personal computer is used both for joint servo control and image processing. Low price CCD camera and capture board are used for generating 100×100 pixels image per $40[ms]$. The target is rotating at a circular trajectory with constant rotational velocity $2\pi[rad/s]$ and radius $100[mm]$. The values selected for the Multirate GPC parameters are $\lambda = 5$, $N_1 = 1$, $N_2 = 8$, $N_u = 8$ and $m = 8$. Fig.11, Fig.12 and Fig.13 show the drastic effectiveness of our proposed intersample predictor. It can compensate the delay of vision sensor without sacrificing the accuracy of tracking trajectory.

5. Conclusion

In this paper, coordinate transformation problem due to the multirate characteristics of visual servo system was explained. A simulation was carried out to examine it. Then a novel approach for high speed visual servo control using intersample predictor based on multirate GPC was presented. The drastic performance of proposed approach was demonstrated through computer simulations and experiments using two-link direct drive robot.

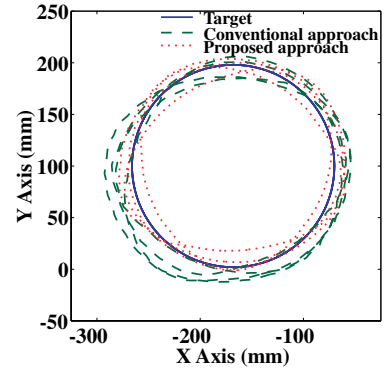


Fig. 11. Tracking trajectory(experiment)

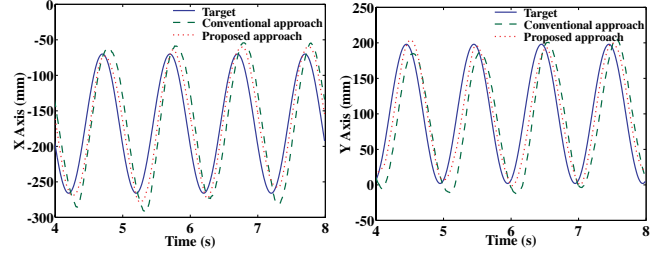


Fig. 12. Tracking response(experiment)

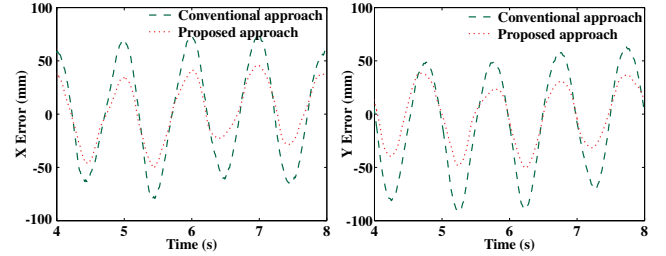


Fig. 13. Tracking error(experiment)

References

- (1) P.I. Corke, Visual Control of Robots: high performance visual servoing, Research Studies Press, 1996.
- (2) K.Hashimoto and H.Kimura, Visual servoing with nonlinear observer, In IEEE Int. Conf. Robotics and Automation pp.484-489,Nagoya,Japan,1995.
- (3) K.Hashimoto and T.Noritsugu, Observer-based control for visual servoing, In 13th IFAC World Congress, Vol.F pp.453-458, San Francisco, 1996.
- (4) J.A. Gangloff, M.de Mathelin and G. Abba, 6 DOF high speed dynamic visual servoing using GPC controllers.In IEEE Int. Conf. Robotics and Automation pp.2008-2013, 1998.
- (5) J.A. Gangloff and M.de Mathelin, High speed visual servoing of a 6 DOF manipulator using MIMO predictive control.In IEEE Int. Conf. Robotics and Automation pp.3751-3756, 2000.
- (6) T.P. Sim, G.S. Hong and K.B. Lim, Multirate predictor control scheme for visual servo control, IEE Proc.-Control Theory Appl., Vol. 149, No. 2, March 2002.
- (7) H. Fujimoto, Y. Hori, High Performance Servo Systems Based on Multirate Sampling Control, IFAC Journal on Control Engineering Practice, vol. 10, no. 7, pp. 773-781, 2002.
- (8) T. Chen and B. Francis, Optimal Sampled-Data Control Systems. Springer, 1995.
- (9) K.V. Ling, K.W. Lim, A State Space GPC with Extensions to Multirate Control, Automatica, Vol. 32, No. 7. pp. 1067-1071, 1996.